Available online at www.sciencedirect.com
SCIENCE DIRECT®
Journal of Electroanalytical Chemistry 544 (2003) 101–106
Journal of Electroanalytical Chemistry
www.elsevier.com/locate/jelechem

Spectroelectrochemistry of palladium hexacyanoferrate films on platinum substrates

Reynaldo O. Lezna [a,*], Roberto Romagnoli [b], Norma R. de Tacconi [c,*], Krishnan Rajeshwar [c]

[a] INIFTA, CONICET-Universidad Nacional de La Plata CC. 16, Suc. 4, La Plata (B1906ZAA), Argentina
[b] CIDEPINT, Centro de investigación y Desarrollo en Tecnología de Pinturas Calle 52 el 121 y 122, La Plata, Argentina
[c] Department of Chemistry and Biochemistry, The University of Texas at Arlington, Arlington, TX 76019-0065, USA

Received 23 September 2002; received in revised form 20 December 2002; accepted 22 January 2003

Abstract

Among the Prussian blue analogs, palladium hexacyanoferrate (PdHCF) is of interest from electrochromic and catalytic perspectives, but has not been extensively studied to date. In this paper we report on the combined use of cyclic voltammetry and in situ infrared and UV–vis spectroelectrochemistry of PdHCF films potentiodynamically grown on platinum electrodes. Infrared spectroscopy (in the cyanide stretching frequency region) showed two pairs of interrelated bands at 2075 cm^{-1}/2180 cm^{-1} and 2110 cm^{-1}/2130 cm^{-1}. UV–vis reflectance spectroscopy also showed two distinct sets of features that are entirely in agreement with the voltammetric peaks and infrared signatures at corresponding potentials. These redox processes have excellent stability and correspond to two PdHCF compound stoichiometries bearing Pd/Fe elemental ratios of 1:1 and 3:2, respectively. A comparison of redox processes and compound stoichiometries in PdHCF with counterparts of Group VIII B metals (namely Ni and Pt) is finally presented.

Keywords: Prussian blue analogs; Electrochromism; Redox transitions; Infrared spectroelectrochemistry; UV–vis reflectance spectroscopy

1. Introduction

Prussian blue and related metal hexacyanoferrates are of interest from both fundamental and practical perspectives [1–4]. These compounds can be generically represented by the formula $A_hB_k[Fe(CN)_6]_l$, where A is usually an alkali metal cation and B is a transition metal. The subscripts h, k, l are stoichiometric coefficients and their values depend on the oxidation states found for the B and Fe redox centers. Renewed interest in these compounds has been spurred by the recent discovery of photomagnetism in the CoFe Prussian blue analogs [4–8]. In this paper, we discuss the spectroelectrochemical behavior of a little-studied member of this family, palladium hexacyanoferrate (PdHCF).

To our knowledge, only two previous reports exist on PdHCF [9,10]. A paper has also appeared on mixed nickel/palladium hexacyanoferrate films [11]. In the first communication, the growth and cyclic voltammetric behavior of films on glassy carbon substrates, were described [9]. Ex situ infrared spectra of PdHCF in the oxidized and reduced states were also presented [9]. A more recent study describes the electroless growth of a Pd layer on an aluminum substrate and its subsequent derivatization to PdHCF [10]. The focus of this latter study was mainly on the influence of varying A cations (Li, Na, K, Rb, Cs) on the electrochemical behavior of PdHCF. In relation to mixed Prussian blue analogs, nickel/palladium hexacyanoferrate composite films were reported to have unique voltammetric and electrochromic characteristics that differ from the corresponding parent members [11].

The present study builds on these two earlier investigations with the use of in situ (UV–vis and IR) spectroscopic probes, coupled with light intensity or

* Corresponding authors. Tel.: +1-817-272-3810; fax: +1-817-272-3808.
E-mail addresses: rolezna@inifta.unlp.edu.ar (R.O. Lezna), ntacconi@uta.edu (N.R. de Tacconi).

0022-0728/03/$ - see front matter © 2003 Elsevier Science B.V. All rights reserved.
doi:10.1016/S0022-0728(03)00081-0

potential modulation of the film in 1 M KCl. Such spectroelectrochemical experiments have shed valuable light on the redox and electrochromic behavior of Prussian blue analogs in general [1,12–19]. It is also of interest to compare the redox signatures and compound stoichiometries in the PdHCF system with the corresponding compounds derived from the other two Group VIII B metals in the Periodic Table, namely Ni and Pt. The two noble metals in the +2 oxidation states have the same nd^8 electron configuration as the Ni case.

2. Experimental

The working electrodes were comprised of polycrystalline Pt disks from Johnson Matthey (99.998%). The electrode diameter was 6.0 mm (geometric area = 0.28 cm^2) for UV–vis spectroelectrochemistry and 10.0 mm (area = 0.78 cm^2) for IR spectroelectrochemical experiments. Prior to each experiment, the working electrode surface was polished to a mirror finish with alumina particles (Buehler) down to 0.05 μm followed by rinsing with Millipore Milli-Q water and sonication. Conventional electrochemical cells with auxiliary ports were used for film growth and cyclic voltammetry (CV). A platinum mesh (separated from the main cell compartment by a porous disk) was used as a counter electrode. The reference electrode was a SCE placed in a separate port and connected to the main cell via a Luggin capillary; potentials are quoted with respect to this reference. All experiments were conducted in 1 M KCl supporting electrolyte, which was carefully de-oxygenated by bubbling purified N_2. All experiments pertain to the laboratory ambient temperature (25 ± 5 °C).

The PdHCF films were potentiodynamically grown on the polished Pt electrodes from solutions made up of 1×10^{-3} M $PdCl_2$ + 1×10^{-3} M $K_3[Fe(CN)_6]$ in de-oxygenated 1 M KCl, that was adjusted to pH ~2.5 with concentrated HCl [9]. Potential scan rates of either 50 or 100 mV s^{-1} were used for film growth within a 0–0.95 V potential window. The number of potentiodynamic cycles (of the order of 300 cycles) was adjusted to accumulate a pre-selected charge (obtained by integration of the anodic voltammetric peaks, see for example, Fig. 1 below) in the range of 10–14 mC cm^{-2}. Taking the latter as the Faradaic charge related to the +2 ↔ +3 interconversion of the iron center in PdHCF, film loadings of 1.0×10^{-7} to 1.5×10^{-7} mol cm^{-2} are obtained. Details of the electrochemical instrumentation are given elsewhere [19].

Infrared spectra were obtained in the 2250 –2000 cm^{-1} range. The working electrode, a flat disc, was placed tightly against a CaF_2 window so as to create a thin (μm) solution layer. IR radiation reaches the electrode surface at an angle of 60°. Details of the IR spectrometer are given elsewhere [19]. The reflected intensity, R, was p-polarized and sensed by a narrow-band, high sensitivity, mercury cadmium telluride detector [19]. Two types of IR spectroelectrochemical experiments were done. In the first, the output signal was chopper-modulated at 80 Hz and the working electrode potential was set at a fixed value during the spectral scan. This procedure was repeated at incrementally increasing (or decreasing) step potential values. In the final spectrum presented, the reflectance signal (after demodulation by a lock-in amplifier) is normalized to the corresponding value at a reference (baseline) potential, R_{ref}; $\Delta R/R_{ref} = (R - R_{ref})/R_{ref}$ [19].

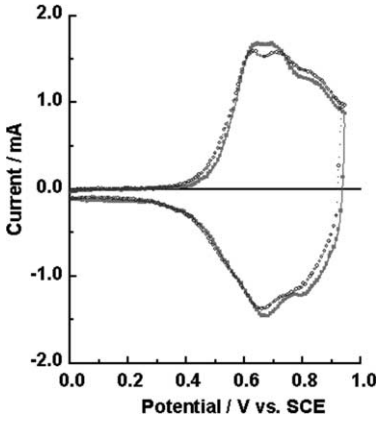

Fig. 1. Cyclic voltammograms for a PdHCF film in 1 M KCl (pH 2.5) for: (■) a freshly prepared film, and (○) the same film after completion of experiments shown in Figs. 2 and 3. Potential scan rate: 50 mV s^{-1}, initial potential: 0.0 V, electrode area: 0.78 cm^2.

The reflected IR light intensity was also modulated by applying a square-wave potential pulse to the working electrode at 11 Hz, and within chosen potentials to span specific redox processes. The resultant ac signal was then processed in a similar manner as above. These two types of IR modulation spectroscopy methods are discussed in detail elsewhere [20,21].

UV–vis spectroelectrochemistry was performed on a custom-built optical multichannel analyser (EG&G PAR OMAIII) fitted with a cooled Si diode array detector (1024 channels, 14-bit resolution). Reflectance spectra were collected rapidly during slow (typically 5 mV s^{-1}) voltammetric scans. Differential spectra of higher sensitivity were obtained by modulating at 11 Hz (modulation amplitude: 50 mV_{p-p}), the modulation being superimposed on a slow (2mV/s) potential ramp. Rectification was done with a lock-in amplifier. Other details are given elsewhere [22–24].

3. Results and discussion

3.1. Cyclic voltammetry of PdHCF in KCl electrolyte

Fig. 1 contains a representative cyclic voltammogram (potential scan rate: 50 mV s^{-1}) of a PdHCF film

supported on Pt in 1 M KCl. This CV profile is in good agreement with that presented by previous authors in the same supporting electrolyte [9] but more complex than that seen in 1 M KNO_3 [10]. Three pairs of redox waves can be discerned under the broad envelope in Fig. 1, a trend also reported by the first group [9]. The CV data served as a basis for choosing the potential step increments for the spectroelectrochemical experiments to be discussed next.

3.2. IR spectroelectrochemistry

Fig. 2 contains normalized in situ IR spectra (in the cyanide stretching region) after the working electrode was stepped to various potentials in the 0–0.95 V potential window. Thus the spectrum at 0.0 V in Fig. 2 represents the reduced state of the PdHCF film and the spectrum at 0.9 V corresponds to the fully oxidized state. The former is characterized by bands at 2075 and 2110 cm^{-1}, while the latter shows these bands at 2130 and 2180 cm^{-1}. Ex situ IR reflectance data were reported in an earlier study [9] with a 2061 cm^{-1} band for the reduced state of the PdHCF film. A 'splitting' of the cyanide stretching band upon oxidation was reported by these authors with the new band appearing at frequencies very close to those observed in the present study (Fig. 2).

The inter-relationship of these two sets of bands corresponding to the reduced and oxidized parent states of PdHCF, is best brought out either in difference spectra or more dynamically (see below) by potential-modulation spectroscopy. Both these types of spectral data are shown in Fig. 3 for the potential windows 0–0.70 V (Fig. 3a), 0–0.80 V (Fig. 3b), and 0–0.90 V (Fig. 3c), respectively. These potential windows encompass the first, second and third pairs of redox features seen in

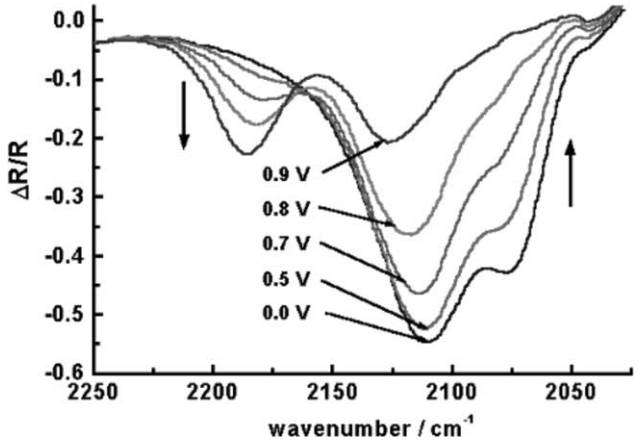

Fig. 2. In situ infrared reflectance spectra of a PdHCF film in 1 M KCl (pH 2.5) at stepwise increasing potentials (0.0, 0.5, 0.7, 0.8, 0.9 V). The reference spectrum corresponding to the platinum electrode without film was subtracted from these scans. Light intensity was chopper modulated at 80 Hz. PdHCF loading: 1.5×10^{-7} mol cm^{-2}.

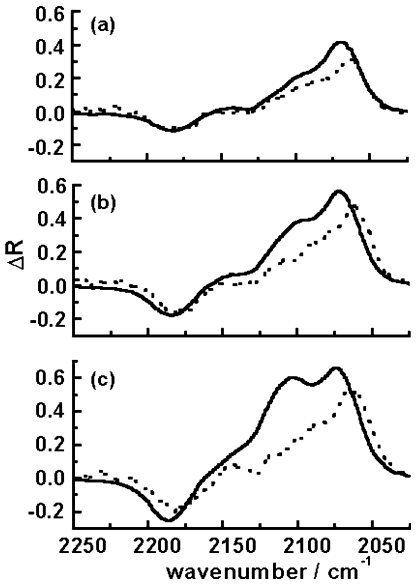

Fig. 3. Comparison of in situ IR difference and modulation spectra obtained in three potential windows: 0–0.70 V (a), 0–0.80 V (b), and 0–0.90 V (c). Difference spectra were obtained by subtracting the steady state spectra at the corresponding potential limits (solid lines), and modulation spectra were recorded under potential pulses of 11 Hz in the same potential range (dashed lines). PdHCF loading as in Fig. 2.

the CV data (cf. Fig. 1). The difference spectra (reconstructed from the corresponding stationary potential spectra, similar to those in Fig. 2) and the modulation spectra are shown as solid and dashed lines in each frame in Fig. 3.

In interpreting spectra as in Fig. 3, it must be borne in mind that that the up-going (positive signals) reflect the dominant contribution from the reduced state of the film. Conversely, the down-going (negative signals) report on the oxidized state of PdHCF. The very different amplitudes in the two cases (cf. also Fig. 2) originate from the vastly different extinction coefficients. Any difference between the two sets of traces in Fig. 3 is attributable to the rather different mode of acquisition of the IR reflectance data. In other words, the lower signal amplitudes in the modulation experiments (i.e. dashed lines) relative to the difference spectra, originate from the fact that only those redox sites that respond to the potential modulation at 11 Hz manifest themselves, unlike the results in the 'stationary' perturbation involved in the potential step experiments. Interestingly, the deviation of the two sets of traces in Fig. 3: (a) manifests most strongly in the intermediate frequency range, $\sim$2110– $\sim$2150 cm^{-1}; and (b) increases markedly as the potential window is made increasingly more positive, cf. Fig. 3a–c. In particular, the output signal in the $\sim$2110–2130 cm^{-1} range appears to be most affected by both the rate of potential change (i.e. whether stationary or dynamic) and the window size. For example, note the progressive switch in the relative contribution of the two up-going signals in

the difference spectra from Fig. 3a–c, so much so that the intermediate frequency feature has evolved from a shoulder in Fig. 3a to almost the same amplitude as the 2075 cm^{-1} band in Fig. 3c.

Based on the data in Figs. 2 and 3, we can tentatively assign the 2075 cm^{-1}/2180 cm^{-1} and the 2110 cm^{-1}/2130 cm^{-1} IR features as redox partners. Specifically, the latter pair corresponds to a charge transfer process that appears to be more sluggish than that corresponding to the 2075 cm^{-1}/2180 cm^{-1} signature. We will speculate on the chemical identities of these participating redox species later in the discussion.

3.3. UV–vis spectroelectrochemistry and electrochromism

Fig. 4 contains difference in situ UV–vis reflectance spectra in the 300–600 nm range; these spectra reflecting the progressive conversion of PdHCF from its reduced (light yellow) to the oxidized (yellow–green) state (Fig. 4a) and back to its reduced state (Fig. 4b) as the potential is cycled in the 0–0.95 V range. These spectra as a function of potential show a quite reversible behavior of the film with very slight deviations between positive and negative potential directions. Once again, the up-going bands in Fig. 4 reflect the contribution from the reduced state of the film and the down-going (positive) bands correspond to the oxidized parent state. These two features peak at 410 and 465 nm, respectively. These difference spectra are more illuminating than their

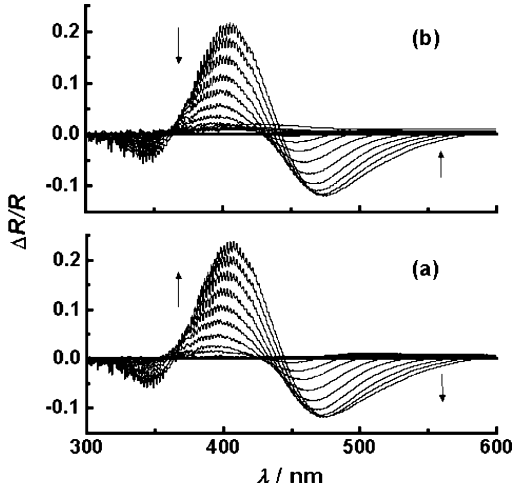

Fig. 4. In situ UV–vis reflectance spectra, $\Delta R/R = [(R - R_{0.0\ V})/R_{0.0\ V}]$, collected every 0.025 V during a cyclic potential sweep at 5 mV s^{-1} in the 0−0.95 V range. For the sake of clarity, only a selected sub-set of spectra are shown for the positive- (a) and negative-going scan directions (b). Spectra were obtained at an incidence angle 45°, with an exposure time of 0.03 s, and were the average of 20 measurements. All spectra are referred to the spectrum at 0.0 V. Electrolyte: 1 M KCl adjusted to pH 2.5. PdHCF loading: 1.1×10^{-7} mol cm^{-2}.

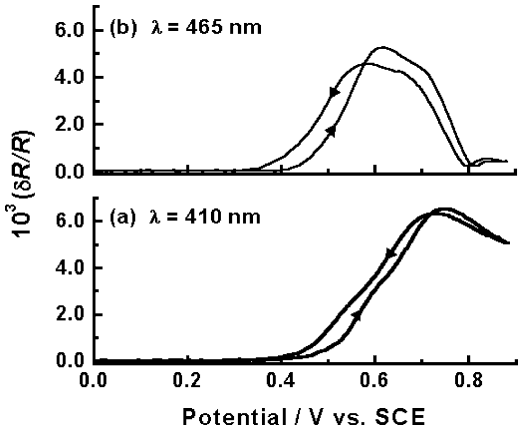

Fig. 5. Cyclic differential UV–vis reflectance (as magnitude) vs. potential obtained for a PdHCF film at 410 nm (reduced state) (a), and 465 nm (oxidized state) (b). Light incidence angle: 45°, modulation frequency: 11 Hz, modulation amplitude: 50 mV_{p-p}, potential scan rate: 2 mV s^{-1}, one cycle. Supporting electrolyte as in Fig. 1. PdHCF loading as in Fig. 4.

absolute counterparts (not shown) because of the large overlap of the spectra in the reduced and oxidized states.

The optical impedance spectra in Fig. 5 allow for the redox processes (leading to color changes) to be examined with greater resolution. As described in Section 2, these data were acquired by modulating the potential at 11 Hz while the film was slowly scanned from 0 to 0.8 V at 2 mV s^{-1}. Both, the in-phase (0°) and quadrature (90°) components of the output signals were monitored separately, the magnitude being shown in Fig. 5. The important point to note with the data in Fig. 5 (relative to Fig. 4) is that two distinct sets of features are seen at potentials up to the ~0.9 V limit, the first associated with redox switching in the 0.55–0.61 V region and the other in the 0.68–0.75 V window. In this regard, the voltammogram in Fig. 1 (with current as the output signal) and the 'reflectogram' in Fig. 5 (with reflectance as the output signal) are entirely in accord with one another.

3.4. Film stability

Fig. 6 illustrates the change in reflectance (at 410 and 465 nm) as the PdHCF film is repeatedly switched between the reduced (light yellow) and the oxidized (yellow–green) states. This process can be repeated over many tens of cycles without any degradation in film response. The data in Fig. 6 provide indications on the excellent chemical and electrochemical (redox) stability of the PdHCF film as long as the potential window is kept within the 0–0.95 V limits. Similar electrochromic reversibility and film stability were reported by previous authors over ~200 switch cycles between 0 and 1.0 V [9]. Other evidence was seen, in terms of both voltammetry and IR data, in this study. Specifically, the cyclic voltammogram of a PdHCF film acquired after the

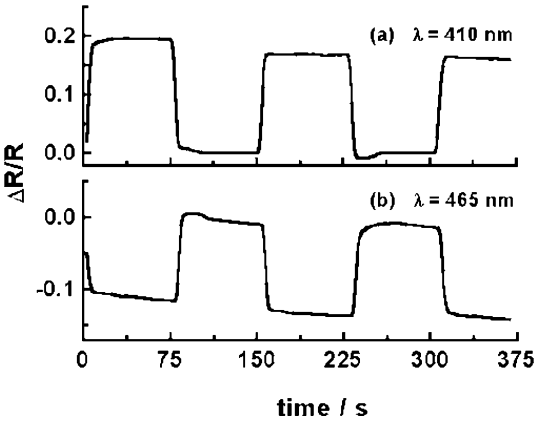

Fig. 6. UV–vis reflectance transients for a PdHCF film subjected to square potential pulses between 0.0 and 0.95 V. (a) 410 nm, and (b) 465 nm. Supporting electrolyte as in Fig. 1. PdHCF loading as in Fig. 4.

experiments in Figs. 2 and 3 were completed, was virtually indistinguishable from that recorded initially (cf. the two CV profiles in Fig. 1). Similarly, a normalized IR spectrum of another PdHCF film (as shown in Fig. 2a) was virtually identical to that obtained after the film was subjected to a series of potential steps from 0 V to varying limits in the 0.5–0.9 V range.

4. General discussion

4.1. Redox electrochemistry in PdHCF and compound stoichiometry

If we assume that Pd exists in the +2 formal oxidation state, then any redox transformation in PdHCF is attributable to the $+2 \leftrightarrow +3$ interconversion of the Fe center in the compound. We can envisage two compound stoichiometries in the PdHCF system, bearing Pd/Fe elemental ratios of either 1:1 or 3:2, i.e. $K_2Pd[Fe(CN)_6]$ or $KPd_{1.5}[Fe(CN)_6]$, respectively. By analogy with other $A_hB_k[Fe(CN)_6]_l$ compounds, these two compounds have structures comprising of Fe and B metal atoms with bridging cyanide groups in a face centered cubic lattice arrangement with the alkali cations occupying the tetrahedral holes in the unit cell. The compound with a Pd/Fe ratio of 3/2 is deficient in the $[Fe(CN)_6]^{3-/4-}$ groups in the lattice and the vacancies are filled with water molecules [4,8]. Redox interconversions including these two compounds are represented by the equations:

$$KPd[Fe(CN)_6] + e^- + K^+ \Leftrightarrow K_2Pd[Fe(CN)_6] \quad (1)$$

$$Pd_{1.5}[Fe(CN)_6] + e^- + K^+ \Leftrightarrow KPd_{1.5}[Fe(CN)_6] \quad (2)$$

We assign the multiple redox waves seen in CV and the two pairs of IR features in the cyanide stretching region to these two compounds. In both Eqs. (1) and (2), reduction of the PdHCF compound is accompanied by K^+ ingress into the structure to maintain charge neutrality. The increase in the ν_{CN} frequency upon compound oxidation is entirely consistent with the trend observed for other $A_hB_k[Fe(CN)_6]_l$ compounds [19,25]. Also by analogy with these other compounds, we tentatively assign the 2075/2180 cm^{-1} IR feature to the 1:1 compound and the 2110/2130 cm^{-1} to the 3:2 counterpart. It then follows from the data presented above, that reaction (1) ($0.55 < E^1_{redox} < 0.61$ V) is kinetically rather more facile relative to reaction (2) ($0.68 < E^2_{redox} < 0.75$ V). This is reasonable considering that the process represented by reaction (2) probably entails more lattice distortion because one of the redox partners, $Pd_{1.5}[Fe(CN)_6]$, completely lacks K^+ cations in its structure. Such effects are known in Prussian blue electrochemistry [26]. It is pointed out that no mention of compound stoichiometry appears in either of the previous studies on PdHCF [9,10]. Further, unlike the case of other $A_hB_k[Fe(CN)_6]_l$ analogs, the solid state chemistry literature of PdHCF appears to be very sparse. Further work on structural and composition aspects of PdHCF (probably also complemented by other methods such as precipitation), while undoubtedly necessary, is beyond the scope of the present spectroelectrochemically-oriented study.

4.2. Comparison with other Group VIII (Ni and Pt) analogs and concluding remarks

The NiHCF analogue has been extensively studied [25,27–37]. Both the 1:1 and the 3:2 compounds appear to be implicated in the electrochemical and spectroelectrochemical investigations and IR data appear for the 3:2 compound stoichiometry in the solid state [37–39]. The ν_{CN} IR feature appears at 2114 cm^{-1} for the reduced state of the compound and it shifts to 2174 cm^{-1} upon oxidation of the Fe(II) redox center [25]. Studies on PtHCF are even more sparse and a preliminary study of this compound [40] invokes only the 1:1 compound stoichiometry. No spectroelectrochemical studies exist, at least to our knowledge, on PtHCF. Similarly, no ex situ IR data appear to exist for PtHCF compounds in the solid state.

The rather simple pattern of compound stoichiometry and redox processes in the Group VIII (Ni, Pd, Pt) family, contrasts sharply with the wide array of compounds in the CoHCF system, studied recently in our laboratories [19]. However, the rather low degree of contrast in the UV–vis spectral signatures for PdHCF in the oxidized and reduced states does not auger well for electrochromic applications of this compound. On the other hand, the intrinsically high electrocatalytic activity of Pd, may render the PdHCF compound attractive for driving catalytic reactions of practical interest.

Acknowledgements

This collaborative project was facilitated by travel funds through the NSF/CONICET International Programs between the US and Argentina. K.R. acknowledges partial financial support from the Texas Higher Education Coordinating Board, Advanced Technology Program.

References

[1] K. Itaya, I. Uchida, V. Neff, Acc. Chem. Res. 19 (1986) 162.
[2] C.G. Granquist, Handbook of Electrochromic Materials, Elsevier, New York, 1995.
[3] P.M.S. Monk, R.J. Mortimer, D.R. Rosseinsky, Electrochromism: Fundamentals and Applications, VCH, Weinheim, 1995.
[4] S.-i. Ohkoshi, K. Hashimoto, J. Photochem. Photobiol. C: Photochem. Rev. 2 (2001) 71.
[5] O. Sato, T. Iyoda, A. Fujishima, K. Hashimoto, Science 272 (1996) 704.
[6] A. Bleuzen, C. Lomenech, V. Escax, F. Villain, F. Varret, Ch. Cartier dit Moulin, M. Verdaguer, J. Am. Chem. Soc. 122 (2000) 6648.
[7] Ch. Cartier dit Moulin, F. Villain, A. Bleuzen, M.A. Arrio, Ph. Sainctavit, C. Lomenech, V. Escax, F. Baudelet, E. Dartyge, J.J. Gallet, M. Verdaguer, J. Am. Chem. Soc 122 (2000) 6653.
[8] The Electrochemical Society Interface, Special Issue on Molecular Magnets, vol. 11, no. 3, 2002.
[9] M. Jiang, Z. Zhao, J. Electroanal. Chem. 292 (1990) 281.
[10] M.H. Pournaghi-Azar, H. Dastang, J. Electroanal. Chem. 523 (2002) 26.
[11] P.J. Kulesza, M.A. Malik, R. Schmidt, A. Smolinska, K. Miecznikowski, S. Zamponi, A. Czerwinski, M. Berrettoni, R. Marassi, J. Electroanal. Chem. 487 (2000) 57.
[12] Z. Gao, G. Wan, P. Li, Z. Zhao, Electrochim. Acta 36 (1991) 147.
[13] P.J. Kulesza, M.A. Malik, S. Zamponi, M. Berretoni, R. Marassi, J. Electroanal. Chem. 397 (1995) 287.
[14] P.J. Kulesza, M.A. Malik, K. Miecznikowski, A. Wolkiewicz, S. Zamponi, M. Berretoni, R. Marassi, J. Electrochem. Soc. 143 (1996) L10.
[15] H.-Q. Zhang, X.-Q. Li, Talanta 44 (1997) 2069.
[16] P.J. Kulesza, S. Zamponi, M.A. Malik, M. Berretoni, A. Wolkiewicz, R. Marassi, Electrochim. Acta 43 (1998) 919.
[17] K. Ogura, K. Nakaoka, M. Nakayama, J. Electroanal. Chem. 486 (2000) 119.
[18] N.R. de Tacconi, K. Rajeshwar, R.O. Lezna, J. Electroanal. Chem. 500 (2001) 270.
[19] R.O. Lezna, R. Romagnoli, N.R. de Tacconi, K. Rajeshwar, J. Phys. Chem. B 106 (2002) 3612.
[20] R.O. Lezna, K. Kunimatsu, T. Ohtsuka, N. Sato, J. Electrochem. Soc. 134 (1987) 3090.
[21] R.O. Lezna, An. Asoc. Quim. Argent. 82 (1994) 293.
[22] R.O. Lezna, N.R. de Tacconi, J.A. Rapallini, A.J. Arvia, An. Asoc. Quim. Argent. 76 (1988) 25.
[23] S. Juanto, R.O. Lezna, A.J. Arvia, Electrochim. Acta 39 (1994) 81.
[24] R.O. Lezna, S. Juanto, J.H. Zagal, J. Electroanal. Chem. 389 (1995) 197.
[25] S. Sinha, B.D. Humphrey, A.B. Bocarsly, Inorg. Chem. 23 (1984) 203.
[26] A. Dostal, G. Kauschka, S.J. Reddy, F. Scholz, J. Electroanal. Chem. 406 (1996) 155.
[27] A.B. Bocarsly, S. Sinha, J. Electroanal. Chem. 137 (1982) 157.
[28] A.B. Bocarsly, S. Sinha, J. Electroanal. Chem. 140 (1982) 167.
[29] S. Sinha, B.D. Humphrey, A.B. Bocarsly, J. Electroanal. Chem. 162 (1984) 351.
[30] B.D. Humphrey, S. Sinha, A.B. Bocarsly, J. Phys. Chem. 91 (1987) 586.
[31] L.J. Amos, A. Duggal, E.I. Mirsky, P. Raganesi, A.B. Bocarsly, P.A. Fitzgerald-Bocarsly, Anal. Chem. 60 (1988) 245.
[32] L.F. Schneemeyer, S.E. Spengler, D.W. Murphy, Inorg. Chem. 24 (1985) 3044.
[33] G. Inzelt, Electroanalysis 7 (1995) 895.
[34] N.R. de Tacconi, J. Carmona, K. Rajeshwar, J. Phys. Chem. B 101 (1997) 10151.
[35] N.R. de Tacconi, J. Carmona, W. Balsam, K. Rajeshwar, Chem. Mater. 10 (1998) 25.
[36] T.R.I. Cataldi, R. Guascito, A.M. Salvi, J. Electroanal. Chem. 417 (1996) 83.
[37] D.-M. Zhou, H.-X. Ju, H.-Y. Chen, J. Electroanal. Chem. 408 (1996) 219.
[38] S.N. Ghosh, J. Inorg. Nucl. Chem. 36 (1974) 2465.
[39] J.B. Ayers, W.H. Waggoner, J. Inorg. Nucl. Chem. 33 (1971) 721.
[40] S. Liu, H. Li, M. Jiang, P. Li, J. Electroanal. Chem. 426 (1997) 27.